2,4-Dichlorophenoxyacetic acid promotes S-nitrosylation and oxidation of actin affecting cytoskeleton and peroxisomal dynamics

Rodríguez-Serrano M [1]*, Pazmiño DM [1]*, Sparkes I[2,3], Rochetti A[2], Hawes C[2], Romero-Puertas MC[1], Sandalio LM[1]

[1] *Departamento de Bioquímica, Biología Celular y Molecular de Plantas, Estación Experimental del Zaidín, CSIC, Apartado 419, 18080 Granada, Spain*

[2]*School of Biological & Medical Sciences, Oxford Brookes University, Oxford, OX3 0BP, UK*

[3] *Present address: Biosciences, College of Life and Environmental Sciences, Geoffrey Pope building University of Exeter, Stocker Road, Exet , EX4 4QD, UK*

*M. Rodríguez-Serrano and D.M. Pazmiño have equally contributed to this work

Corresponding author:

[1]*Dr. Luisa M. Sandalio*

Telephone: 34 958 181600 (ext 316)

e-mail: luisamaria.sandalio@eez.csic.es;

Running tittle: 2,4-D disturbs actin cytoskeleton by post-translational modifications

Date of submission: 3 February 2014-02-03 Resubmission: 2014-10-04

Number of tables: 0

Number of figures: 6 (Fig. 1 and Fig. 2 in colour; Fig. 3-6 in black and white)

Total word (including references and Figure legends): 8,294

Supplementary figures: 3 (in colour)

Supplementary tables: 0

Supplementary videos: 4

Cover image: 1

Abstract

2,4-Dichlorophenoxyacetic acid (2,4-D) is a synthetic auxin used as a herbicide to control weeds in agriculture. High concentration of 2,4-D promotes leaf epinasty and cell death. In this work, the molecular mechanisms involved in the toxicity of this herbicide are studied by analysing in Arabidopsis plants the accumulation of reactive oxygen species (ROS), nitric oxide (NO) and their effect on cytoskeleton structure and peroxisome dynamics. 2,4-D (23 mM) promotes leaf epinasty, whereas this process was prevented by EDTA, which can reduced ·OH accumulation. The analysis of ROS accumulation by confocal microscopy, showed a 2,4-D-dependent increase of both H_2O_2 and $O_2^{\cdot-}$ while total NO was not affected by the treatment. The herbicide promotes disturbances on the actin cytoskeleton structure as result of post-translational modification of actin by oxidation and *S*-nitrosylation, which could disturb actin polymerization, as suggested by the reduction of the F-actin/G-actin ratio. These effects were reduced by EDTA and the reduction of ROS production in Arabidopsis mutants deficient in xanthine dehydrogenase (*Atxdh*) gave rise a reduction of actin oxidation. Also, 2,4-D alters the dynamics of the peroxisome, slowing the speed and shortening the length of distances run by these organelles. We conclude that 2,4-D promotes oxidative and nitrosative stress, causing disturbances in the actin cytoskeleton, thereby affecting the dynamics of peroxisomes and some other organelles such as mitochondria, XDH being involved in ROS production under these conditions. These structural changes in turn appear to be responsible for the leaf epinasty.

Key words: 2,4-D; actin; cytoskeleton; nitric oxide; peroxisomes; ROS; *S*-nitrosylation; xanthine dehydrogenase.

Abbreviations:

ACX: Acyl CoA oxidase

BR: brassinosteroids

CFP: cyan fluorescent protein

2,4-D: 2,4-dichlorophenoxyacetic acid

cPTIO: 2-(4-carboxyphenyl)-4,4,5,5-tetramethylimidazoline-1-oxyl-3-oxide

DAB: 3,3'-diaminobenzidine

DAF-2: 4,5-diaminofluorescein

DMSO: dimethyl sulfoxide acid

DCF-DA: 2',7'-dichlorodihydrofluorescein diacetate

DNPH: 2,4-dinitrophenylhydrazine

DHE: dihydroethidium

FABD2: actin-binding domain 2 of fimbrin

GFP: green fluorescent protein

HRP: horseradish peroxidase

IAA: auxin

IPA: Immobilized Protein A

Lat B: Latrunculin B

ROS: reactive oxygen species

SOD: superoxide dismutase

TIBA: 2,3,5-triiodobenzoic acid

YFP: yellow fluorescent protein

XDH: xanthine dehydrogenase

XOD: xanthine oxidase

INTRODUCTION

Auxin herbicides have been one of the most successful chemicals used to control weeds in agriculture. 2,4-dichlorophenoxyacetic acid (2,4-D) was the first synthetic auxin analogue to indole-3-acetic acid (IAA, natural auxin) used in agriculture (Grossmann, 2000). The dose-dependent mode of action of 2,4-D causes different effects on sensitive species, and this marks the difference between its action as a growth promoter or as a herbicide. Thus, at low concentrations, 2,4-D stimulates growth and developmental processes, but at high concentrations upsets normal growth and provokes lethal damage in the plant (Grossmann, 2000).Common visual effects induced by 2,4-D and auxin herbicides are epinastic deformations, stem curvature, senescence, and growth inhibition of roots and shoots (Grossmann *et al*. 2001; Pazmiño *et al*., 2012). Pea plants exposed to 2,4-D also develop oxidative-stress symptoms characterized by H_2O_2 over-accumulation, lipid peroxidation, protein oxidation, and the induction of proteolysis (Romero-Puertas *et al*., 2004a; Pazmiño *et al*., 2011; Pazmiño *et al*, 2012). In young leaves ROS accumulation is involved in 2,4-D-induced epinasty, while in adult leaves ROS overproduction triggers senescence (Pazmiño *et al*., 2011). Peroxisomes have been identified as one of the main sources involved in ROS production in response to 2,4-D by the activation of xanthine oxidase and acyl CoA oxidase (Romero-Puertas *et al*., 2004a; Pazmiño *et al*., 2011 and 2014). Peroxisomes are subcellular organelles delimited by a single membrane that contain, as basic enzymatic constituents, catalase and hydrogen peroxide (H_2O_2)-producing flavin oxidases, and occur in almost all eukaryotic cells (Sandalio et al 2013). Peroxisomes can change their enzymatic composition, shape, size, number, and motility depending on the tissue and environmental conditions (Rodríguez-Serrano *et al*., 2009; Sandalio *et al*., 2013).

ROS have a double, antagonistic function in the cells depending on their concentration. That is, at low concentrations, ROS, and particularly H_2O_2, can act as signal molecules and regulate the expression of a large number of genes involved in cell response to different stress conditions and development (Mittler *et al*., 2011). However, high accumulation of ROS is dangerous because it promotes oxidative damage to proteins, lipids, and nucleic acids. Oxidative damages have been demonstrated to be involved in the toxicity mechanisms of different abiotic factors (Sandalio *et al*., 2012; Suzuki *et al*., 2011).

In plants, NO is a key signalling molecule involved in several physiological processes from development to defence responses to both biotic and abiotic stress (Delledonne 2005; Neill *et al*., 2008; del Río, 2011; Astier *et al*., 2011; Yemets *et al*., 2011). NO can regulate diverse biological processes by directly altering proteins through oxidization, nitration or nitrosylation (Zaninotto *et al*., 2006; Astier *et al*. 2011; Vandelle & Delledonne, 2011). *S*-nitrosylation refers to the binding of a NO group to a cysteine residue and can play a significant role in NO-mediated signalling (Stamler *et al.,* 2001; Astier *et al*., 2011; Romero-Puertas *et al*., 2013).

In vivo visualization of actin filaments in cells has allowed to study the numerous roles of the actin cytoskeleton in different process in the cells. These studies have been carried out by using specific actin reporters such as the fusion protein between green fluorescent protein (GFP) and the second actin-binding domain (FABD2) of Arabidopsis fimbrin, AtFIM1 (GFP-FABD2; Sheahan et al., 2004). The cytoskeleton governs important cell processes such as cell division and growth, vesicle transport, organelles movement, and the response of the cell to a wide range of stimuli such as light, gravity, phytohormones, pathogen or wounding (Wasteneys & Yang, 2004; Yemets *et al*., 2011; Lanza *et al*., 2012; Song *et al*., 2012; Sheremet *et al.,* 2012). The cytoskeleton has also been suggested to be one of the major targets of signaling events (Wasteneys & Yang, 2004). Recently, it has been demonstrated that the actin cytoskeleton can acts as a node of convergence in brassinosteroids and auxin signaling by regulating the bundling of actin filaments (Lanza *et al*., 2012). A large body of evidence shows that the actin cytoskeleton plays an important role in the regulation and execution of cell expansion (Baluska *et al*., 2001; Ketelaar *et al*., 2004; Collings *et al.*, 2006). Dynamic actin cytoskeleton rearrangements are regulated by a pool of actin-binding proteins, which sense environmental changes and modulate the actin cytoskeleton through various biochemical activities (Hussey *et al*., 2006; Staiger & Blanchoin, 2006; Staiger *et al*., 2009). A number of drugs and herbicides such as dinitroanilines, benzoic acids, phosphoroamidates, pyridines and carbamates, use the cytoskeleton as a target affecting microtubules in plant cells (Ovidi *et al*., 2001; Blume *et al.*, 2003; Délye *et al*., 2004). Most of these compounds alter polymerization or binding site properties of tubulin heterodimers, although the molecular mechanism is not well known (Délye *et al*.,

2004). Rahman *et al.* (2007) observed that 2,4-D and naphthylphtalamic acid removed actin and slowed down cytoplasmic streaming, although the mechanism involved was not specified. Proteomics studies have shown that plant cytoskeletal proteins can undergo many post-translational modifications including phosphorylation, *S*-glutathionylation, nitration and *S*-nitrosylation, although their functional role and physiological relevance has yet to be elucidated (Yemets *et al.,* 2011).

For this reason, in this work we analysed the effect of 2,4-dichlorophenoxy acetic acid on actin cytoskeleton structure and the mobility of peroxisomes and mitochondria as well as the effect of post-translational modifications of actin by oxidation and S-nitrosylation. The accumulation of reactive oxygen species (H_2O_2 and $O_2^{\cdot-}$) and NO induced by 2,4-D is also studied by *in vivo* confocal imaging. We report that 2,4-D considerably affects the actin cytoskeleton by inducing oxidative and *S*-nitrosylated modifications on the actin, disturbing actin polymerization and compromising the dynamics of peroxisomes and mitochondria.

MATERIALS AND METHODS

Chemicals and plant materials

Arabidopsis thaliana (L.) ecotype Columbia was germinated after 48 h incubation at 4°C, and plants were grown in compost at 22ºC, 16 h light, and 8 h darkness for three weeks. To study the effect of 2,4-dichlorophenoxyacetic acid on Arabidopsis plants, the plants were sprayed once with a 23 mM 2,4-D solution (prepared in 1% dimethyl sulfoxide acid, DMSO) and kept for 72 h until analysed. Control plants were sprayed with the same concentration of DMSO used to prepare 2,4-D. The treatment time and 2,4-D concentration used in this work has been previously optimised in pea plants (Romero-Puertas *et al*., 2004a). The effect of EDTA (10 mM) on Arabidopsis leaves was studied by spraying the chemical 24 h before 2,4-D treatment and the application was repeated with 2,4-D spray. To study the effect of 2,4-D on peroxisome movement, Arabidopsis lines expressing the fusion protein between GFP and the peroxisomal targeting signal SKL from the hydroxypyruvate reductase were used (GFP-SKL; Rodríguez-Serrano *et al*., 2009). The actin cytoskeleton was imaged by using Arabidopsis line expressing the fusion protein GFP-FABD2 (Sheahan *et al*., 2004). Arabidopsis lines expressing simultaneously cyan fluorescent protein (CFP) and yellow fluorescent protein (YFP) associated to peroxisomes and mitochondria, respectively, were obtained by cross pollinating Arabidopsis marker lines px-ck and mt-yk (Nelson *et al*., 2007) and selecting homozygous double lines. Arabidopsis *Atxdh* mutants were supplied by Dr Sagi (Ben-Gurion University, Beer Sheva, Israel) and homozygous lines were selected by analysing XDH activity by native-PAGE and nitro blue tetrazolium staining (Pazmiño *et al*., 2014).

Confocal microscopy

Transgenic Arabidopsis leaves were sliced with razor blades and mounted between a slide and a coverslip in PBS/glycerol 70%. Sections were examined using a Leica confocal laser scanning microscope, Model TCS SL (Leica Microsystems, Wetzlar, Germany). Digital images were made across the epidermal cells. The movement of individual peroxisome stacks was analysed using the classification and particle-tracking routine of Volocity version 3.0 (Improvision; Perkin-Elmer, Palo Alto, CA, USA). This software can track the

movement of individual fluorescent particles in time-resolved two or three dimensions, and automatically generates the speed and track length. For the speed analysis, the images were acquired in the x, y, z and t dimensions. Each movie contained 15 Z series each containing 6-9 frames in the Z axis (1μm interval; 512x512 of resolution and bidirectional scan mode). The movies were generated taking 20 frames in the x, y and t dimension with a 1024x1024 resolution. Quick-time movies of peroxisome movement were generated from sequential images (five frames per second). Arabidopsis plants expressing the fusion protein GFP-FABD2 were used to visualize the actin cytoskeleton. Images of GFP expressing cells were adquired as a z-series with 1 μm interval using a Leica confocal laser scanning microscope (Exc/Em: 488/508) and at different time of 2,4-D (23 mM) treatment (1h, 24 h, 47 h and 72 h). The effect of 25 μM Latrunculin B (Lat B, an inhibitor of actin polymerization, prepared in 0,2% DMSO) on the actin cytoskeleton was also studied in GFP-FABD2 Arabidopsis plants treated with these compounds for 45 min.

Analysis of H_2O_2 and NO in plants extracts

The H_2O_2 concentration was determined in acid extracts from Arabidopsis leaves by spectrofluorimetry as described by Pazmiño *et al*. (2011). All processes were conducted at 4ºC. Leaves (0.5 g) were extracted with 1.5 ml of 1 M $HClO_4$, in presence of insoluble PVP (5%) and centrifuged at 12,000× *g* for 10 min (4 ºC) and the supernatant was filtered through a 0.45-μm Millipore filter. The pH was adjusted to 7.0 with 5 M K_2CO_3 and the filtrate was finally centrifuged at 12,000×*g* for 2 min to remove $KClO_4$. The supernatant was used to measure the H_2O_2 by spectrofluorimetry using homovanillinic acid (Ex/Em: 325/425 nm) and horseradish peroxidase (HRP).

Nitric oxide (NO) was analysed by fluorimetry using 4,5-diaminofluorescein (DAF-2), as described by Nakatsubo *et al*. (1998). After treatment with 2,4-D, leaf extracts were made and incubated with DAF-2 in buffer Hepes 50 mM, pH 7.5 for 2h at 37ºC. Afterwards, NO was measured by analysing DAF-2 fluorescence (Ex/Em: 495/515 nm).

ROS and NO detection by confocal laser scanning fluorescence microscopy

Reactive oxygen species and NO accumulation were imaged by confocal laser scanning microscopy (CLSM). Superoxide radicals were detected by incubating leaf sections with 10 µM dihydroethidium (DHE; Fluka, Buchs, Switzerland; Ex/Em: 450–490/ 520 nm) in 10 mM Tris-HCl (pH 7.4), for 30 min at 37ºC, as indicated by Sandalio *et al*. (2008). Hydrogen peroxide was detected by using 2',7'-dichlorodihydrofluorescein diacetate (DCF-DA) in 10 mM Tris-HCl (pH 7.4) for 30 min at 37ºC and NO with 4,5-diaminofluorescein diacetate (DAF-2DA) for 1h at 25ºC as indicated by Sandalio *et al*. (2008). As negative control 2-(4-carboxyphenyl)-4,4,5,5-tetramethylimidazoline-1-oxyl-3-oxide (cPTIO; 2 mM) was used as NO scavenger. After leaves were embedded in 30% (w/v) polyacrylamide blocks, sections were cut by a vibratome and mounted for examination with a confocal laser scanning microscope (Leica TCS SL; Leica Microsystems). Fluorescence was quantified using LAS AF Leica software and expressed as arbitrary units.

Histochemical analyses

For histochemical analyses of hydrogen peroxide leaves from control and 2,4-D-treated plants were excised and immersed in a 1% solution of 3,3'-diaminobenzidine (DAB) in 10 mM MES buffer (pH 6.5), vacuum-infiltrated for 5 min and then incubated at room temperature for 8 h in the absence of light. Leaves were illuminated until the appearance of brown spots characteristic of the reaction of DAB with H_2O_2. Leaves were bleached by immersion in boiling ethanol to visualize the brown spots (Romero-Puertas *et al*., 2004b). Cell death was evaluated by histochemical analysis using Trypan Blue (Koch & Slusarenko, 1990) at different time of treatment.

Western blot analysis

To analyse the effect of 2,4-D on GFP-fimbrin and actin expression, leaves were homogenized in buffer containing 50 mM Tris-HCl (pH 7.8), 0.1 mM EDTA, (0.2% V/V) Triton X-100 and protease inhibitors cocktail (Sigma, St. Louis, MO, USA). Homogenates were centrifuged at 16,000 g for 30 min at 4 ºC. Equal amount of proteins were loaded into SDS-PAGE (12% acrylamide) and transferred onto polyvinylidene fluoride (PVDF) membrane (Millipore Co.,

Bedford, MA, USA) in a Bio-Rad Semi-Dry Transfer Cell (Bio-Rad, Hercules, CA, USA). GFP was detected using monoclonal antibody anti-GFP (Clontech; 1/10.000 dilution) and goat anti mouse IgG conjugated with horse radish peroxidase (HPR) as secondary antibody (Bio-Rad; 1/ 10.000 dilution). Actin was detected using a specific polyclonal antibody (1/1000 dilution, Molecular Probes^{TM}) and IgG anti-rabbit-HRP (Bio-Rad; 1/10.000 dilution). To analyse the total amount of filamentous actin (F-actin) *versus* free globular actin (G-actin) leaves were homogenized in buffer containing 0.1 M PIPES (pH 6.9) 30% (v/v) glycerol, 5% (w/v) DMSO, 1 mM $NgSO_4$, 1 mM EGTA, 1% (v/v) Triton X-100, 1 mM ATP, and protease inhibitors cocktail. Homogenates were centrifuged at 16.000g for 75 min at 4º C to separate F-actin from G-actin. F-actin from the pellet was depolymerized with cytochalasin and solubilized in equal volume of supernatant containing 0.1 M PIPES (pH 6.9), 1 mM $MgSO_4$, 10 mM $CaCl_2$, and 5 µM cytochalasin D. After incubation for 1 h, equals volumes of both fractions were analyzed by western blot using specific antibody against actin as mentioned above (Rasmussen *et al*., 2010).

Immunochemical detection of *S*-nitrosylated actin

S-nitrosylated proteins were detected following the biotin-switch method that converts -SNO into biotinylated groups (Jaffrey *et al*., 2001). Arabidopsis leaves were homogenized in MAE buffer (25 mM HEPES, 1 mM EDTA, 0.1 mM neocuproine, 0.2 % Triton X-100, pH 7.7) containing complete protease inhibitor cocktail (Sigma, St. Louis, MO, USA). The extract was centrifuged at 4°C for 30 min. Proteins were then assayed with the biotin-switch method. Briefly, equal amount of protein (300µg) from control and treated plant leaf extracts were subjected to the biotin-switch assay (Ortega-Galisteo *et al*., 2012) and biotinylated proteins were purified by immunoprecipitation overnight at 4ºC with 15 µL IPA (UltralLink Immobilized Protein A/G Pierce)/mg of protein and preincubated with 2µL of anti-biotin antibody (Sigma). Beads were washed three times with PBS, and bound proteins were eluated with 10 mM DTT in SDS-PAGE solubilization buffer, loaded in 12% SDS-PAGE, transferred to a PVDF membrane and actin was detected with specific antibodies (1/1000 dilution, Molecular Probes^{TM}).

Immunochemical detection of oxidative modified actin

The proteins containing carbonyl groups were identified as described by Romero-Puertas *et al.* (2002). Equal amount of proteins (500 μg) from leaf extracts were derivatized with 10 mM 2,4-dinitrophenylhydrazine (DNPH; Sigma-Aldrich Co., St Louis, MO, USA) and immunoprecipitated with antibodies against DNP linked to IPA overnight at 4ºC. Oxidized-purified proteins (10 μl) were subjected to SDS-PAGE (12% acrylamide) and transferred onto PVDF membranes as mentioned above. Actin was detected using specific antibodies (1/1000 dilution, Molecular Probes^{TM}).

Protein and statistical analysis

Protein concentration was determined with the BIO-RAD Bradford Protein Assay kit (BIO-RAD) using bovine serum albumin (BSA) as standard. Data were subjected to one-way analysis of variance for each parameter. When the effect was significant ($P<0.05$), differences among means were evaluated for significance by Duncan's multiple-range test ($P< 0.05$).

RESULTS

Effect of 2,4-D on Arabidopsis leaf phenotype and oxygen and nitrogen reactive species accumulation

In previous work carried out in our laboratory, the concentration of the herbicide 2,4-D and the time of treatment was optimized in order to visualize its toxic effects on pea plants, with 23 mM 2,4-D and 72h of treatment being the experimental conditions selected (Romero-Puertas *et al*., 2004a). Therefore we used these conditions to carry out the experiments in Arabidopsis plants. The supply of 23 mM 2,4-D to Arabidopsis plants produced a severe curling or epinasty of rosette leaves, loss of leaf turgidity, and curling of the flower stem which started after 1 h reaching a maximum after 72 h of treatment (Fig.1A, Figure S1). This effect was reduced by the treatment with EDTA as we have shown in previous work on pea leaves (Pazmiño *et al*., 2011; Pazmiño *et al*., 2014).

The analysis of total H_2O_2 in Arabidopsis leaf extracts after treatment with 2,4-D shows a two-fold increase of H_2O_2 (Fig. 2A). By using histochemistry with DAB, we detected a strong increase of H_2O_2 in 2,4-D-treated plants in comparison with untreated plants, the highest accumulation being registered in vascular tissues (Figure S1B). The accumulation of H_2O_2 was also studied in leaf cross sections using DCF-DA and confocal laser microscopy. 2,4-D induced an increase in DCF fluorescence, associated mainly with mesophyll cells, although an increase in fluorescence in secondary veins also appeared in 2,4-D-treated leaves (Fig. 2B and C).The analysis of $O_2^{\cdot-}$ in cross sections of Arabidopsis leaves showed an induction of $O_2^{\cdot-}$ by the herbicide (Fig. 2 D and E) which was reversed by incubation with superoxide dismutase (SOD; data not shown). The $O_2^{\cdot-}$ accumulated in the main and secondary veins, but also in mesophyll and epidermal cells (Fig. 2D and Figure S2). A higher magnification of mesophyll cells revealed the $O_2^{\cdot-}$-dependent fluorescence associated mainly in small puncta which could represent localisation to small organelles such as mitochondria and peroxisomes, while neither chloroplasts nor plasma membrane show any DHE signal (Figure S2). In turn, the image of NO accumulation displayed by DAF-2D fluorescence showed no apparent differences by the treatment with 2,4-D in terms of total NO accumulation, although a slight increase in fluorescence was observed in the epidermis (Fig. 2F and G). The NO scavenger cPTIO was used as

a negative control, showing a considerably reduction of DAF-2DA fluorescence (Fig. 2F and G). NO production was analysed using spectrofluorimetry in order to quantify changes in NO accumulation by the herbicide, but no changes were found in comparison with the values in untreated plants (Fig. 2H).

2,4-D disturbs the actin cytoskeleton by post-translational changes of actin

Recently Raman *et al*. (2007) have shown that 2,4-D can affect actin cytoskeleton structure, although the mechanism involved has not been established so far. To go in depth in this study we analysed the effect of this chemical on the structure of the actin cytoskeleton over the time by using a transgenic Arabidopsis line expressing GFP associated to an actin binding protein (GFP-FABD2; Sheahan *et al.*, 2004). The analysis revealed a slight but not significant reduction of GFP associated to actin filaments after 1 h of treatment, and after 24 h a significant reduction was observed. The maximum effect was observed after 72h, which revealed a reduction in the number and thickness of actin filaments (Fig. 3A). EDTA prevented the disturbances of the actin cytoskeleton organization (Fig. 3B) in the same way as it prevented epinasty. To characterise the disturbances of the actin cytoskeleton induced by 2,4-D, GFP-FABD2 plants were treated with Lat B, which is a well known inhibitor of actin polymerization (Sheahan *et a.l*, 2004). Lat B produced a severe reduction in most of the filamentous actin after 45 min of treatment showing a similar image to that observed with 2,4-D, which suggests that the changes observed in the actin filament network induced by this herbicide could be due to a reduction in the ability of actin to polymerizae (Fig. 3C). This fact was studied by analyzing the content of G-actin and F-actin in leaf extracts at different times of treatment. A statistically significant reduction in the F/G actin ratio was observed after 24 h of treatment, being maximum after 72 h of treatment (Fig. 3D). To study if the disturbances in the actin cytoskeleton is associated with cell death, leaves of Arabidopsis plants were stained with Trypan Blue, a marker of cell viability, at different period of treatment (24, 48 and 72 h). The results obtained did not show any cell death due to the treatment with 2,4-D even after 72 h of treatment (Figure S3). In addition to this, to rule out degradation processes affecting GFP-FABD2 during the treatment with 2,4-D, a Western blot analysis was carried out using a monoclonal anti-GFP antibody. The results

obtained shown that the content of GFP-FABD2 was not affected by the treatment with 2,4-D for 72 h (Fig. 3E). The total actin present in extracts was also analysed by Western blot using specific antibodies against actin. No differences were detected in terms of total protein between control and 2,4-D-treated plants after 72 h of treatment, demonstrating that actin is not down-regulated or proteolitically degraded by the 2,4-D treatment (Fig. 3F). The same results were obtained in plants treated with EDTA. In previous work we have demonstrated that xanthine oxidoreductase (XOD/XDH) is involved in ROS production induced by 2,4-D (Pazmiño *et al*., 2014), and Arabidopsis mutants deficient in this protein (*Atxdh*) show a significant reduction of epinasty induced by 2,4-D, for this reason we analysed the effect of 2,4-D on the content of actin in this mutant. No differences were observed between WT and *Atxdh* (Fig. 3F). To study the cause of 2,4-D-dependent disturbances in the structure of the actin cytoskeleton, we analysed post-translational modifications of actin by oxidation and *S*-nitrosylation after 72 h of 2,4-D exposure. Leaf extracts from WT and *Atxdh* plants treated with 2,4-D for 72 h were incubated with 10 mM DNPH and oxidized proteins containing carbonyl groups were purified by immunoprecipitation using antibodies against DNP linked to Immobilized Protein A (IPA) and actin was visualized by Western blot using a specific antibody. The results obtained revealed a strong increase in the oxidized actin in 2,4-D-treated plants which was considerably reduced in *Atxdh* lines and WT treated with EDTA (Fig. 4A). These results indicate that ROS production stimulated by 2,4-D, is involved in oxidative alterations of actin, which in turn would promote disturbances in the actin cytoskeleton ultrastructure. Actin reportedly undergoes *S*-nitrosylation in both animal and plant tissue, and in animal tissue this change has been demonstrated to affect the rate of actin polymerization under oxidative stress (Dalle-Donne *et al*., 2000). Therefore, *S*-nitrosylated proteins from Arabidopsis leaf extracts were analysed by the biotin-switch method and purified by immunoprecipitation using anti-biotin antibody-IPA, and actin was identified with specific antibodies. The treatment with 2,4-D boosted the content of *S*-nitrosylated actin in comparison with untreated control plants and EDTA significantly reduced it (Fig. 4B).

Peroxisomal dynamics is affected by 2,4-D

Because peroxisomes move along the actin cytoskeleton (Mano *et al.,* 2002; Van Gestel *et al*., 2002) the dynamics of these organelle under 2,4-D toxicity was studied. Peroxisome movement in epidermal cells was assessed after 72 h of treatment. The herbicide caused a two-fold reduction of speed (Fig. 5A) and a reduction of the displacement rate of these organelles (Fig. 5 B). Movies of control and 2,4-D-treated plants showing differences in the dynamics of peroxisomes is provided in video S1 A-B and S 2A-B. As mentioned previously EDTA can reduced the disturbances of actin cytoskeleton induced by 2,4-D, and therefore the role of EDTA in peroxisomal movement was also investigated. The treatment with EDTA reversed the effect of 2,4-D on both the speed and displacement of peroxisomes, reaching values similar to those of the untreated leaves (Fig. 5A and B). In order to know if the effect of 2,4-D is specific for peroxisomes, or is a general effect on organelles motility we analysed the effect of 2,4-D on the movement of mitochondria in Arabidopsis lines expressing YFP in mitochondria and CFP associated to peroxisomes The dynamics of mitochondria was also disturbed by the herbicide showing severe reduction on their motility (Video S 2A-B).

DISCUSSION

Auxins regulate a number of processes related to development and growth in plants, being involved in cell elongation, tissue differentiation, tissue polarity or leaf expansion (Benjamins & Scheres, 2008; Delker *et al*., 2008). 2,4-dichlorophenoxyacetic acid is a synthetic auxin specific for dicotyledons and is considered to be among the most successful herbicides used in agriculture (Grossmann, 2000; Pazmiño *et al*., 2012). One of the most characteristic effects of 2,4-D on sensitive plants is the development of epinasty and stem curvature, as well as reduction of root and stem growth (Grossmann, 2000; Pazmiño *et al*., 2011 and 2012). Different studies have demonstrated that the toxicity of this herbicide is mediated by uncoupling oxidative phosphorylation, changes in the plasma-membrane potential, or oxidative stress (Grossmann *et al*., 2001; Pazmiño *et al*., 2012). Recently, we have demonstrated that ROS are involved in

the toxicity of 2,4-D being responsible for both the epinasty and senescence induced by this herbicide (Pazmiño *et al*., 2011; 2014). The analysis of different sources of ROS under 2,4-D toxicity point to xanthine oxidoreductase (XOD/XDH) and Acyl CoA oxidase (ACX) as the main agents responsible for 2,4-D-imposed oxidative stress (Pazmiño *et al.*, 2011 and 2014). Both enzymes are components of peroxisomes, which are characterized by a strong oxidative metabolism (Sandalio *et al*., 2013). The role of peroxisomes in ROS and NO metabolism has recently been demonstrated and the importance of these molecules in signalling has been elucidated over the past ten years (Vandenabeele *et al*., 2004; del Río 2011; Ortega-Galisteo *et al*., 2012; Sandalio *et al*., 2013). The rate of ROS accumulation would define the role of these reactive species as signal molecules (low production) or as dangerous compounds (high accumulation) (Mittler *et al*., 2011; Sandalio *et al*., 2013). In turn, NO can interfere with signal-transduction pathways or can modify proteins, modulating their activities or properties (Moreau *et al*., 2010). The analysis of H_2O_2 accumulation by different methods showed that 2,4-D induced the over-accumulation of this ROS, which in turn caused oxidative alteration of proteins, as we demonstrated recently by carbonyl content analyses (Pazmiño *et al*., 2014). One of the target proteins of this oxidative modification was actin. Concerning the main sources of ROS under these conditions, the analyses of ROS accumulation by confocal laser microscopy suggest that peroxisomes and mitochondria may be the main cell compartments involved in ROS production. Recently, we have reported the production of H_2O_2 in peroxisomes induced by 2,4-D in tobacco leaves transiently expressing the biosensor HyperAs-SKL in peroxisomes and pea leaf peroxisomes (Sandalio *et al.*, 2013; Pazmiño *et al*., 2014). The generation of ROS and particularly ·OH is a prerequisite for cell-wall loosening and normal growth (Schopfer *et al*., 2002; Liszkay *et al*., 2004) and under the conditions used in this work, 2,4-D could promote over-accumulation of these species, which in turn could trigger cell malformation, leading to epinasty, a hypothesis supported by the protective role of EDTA which can act as a metal chelator, avoiding Fenton-type reactions and also reacts directly with ·OH at a rate constant of 2.8×10^{-9} (Halliwell & Gutteridge, 2000).

The plants treated with 2,4-D showed a strong reduction in actin bundling and polymerization, which increase with the time of treatment and was

completely prevented by EDTA. EDTA also prevented epinasty, demonstrating that the cytoskeletal disturbances are involved in the development of this phenotype. The protective effect of EDTA was due mainly to the reduction of actin oxidation. Recently we have observed that EDTA reduce oxidation of proteins in Arabidopsis plants treated with 2,4-D (Pazmiño *et al*., 2014) and also reduced the accumulation of H_2O_2 induced by 2,4-D in pea shoots (Pazmiño et al., 2014). These results suggest that ·OH is the main ROS involved in the actin cytoskeleton disturbances and the results obtained with *Atxdh* plants suggest that XOD/XDH are partially involved in the production of this ROS. In addition to ROS, NO is also a key molecule involved in signalling and controlling functionality of different proteins by combining with cysteines and giving rise to *S*-nitrosylation of proteins. Despite the absence of changes in total NO accumulation, an increase of *S*-nitrosylation of actin was observed in 2,4-D-treated plants when *S*-nitrosylated proteins were purified. A reduction of *S*-nitrosylation was observed when 2,4-D plants were pre-treated with EDTA however. It appears that this decrease it is not metal dependent as EDTA would favour and protect S-nitrosylation (Jaffrey *et al*., 2001). Other molecules however, could regulate also this post-translational modification, such as ascorbate or glutathione which concentration is altered by EDTA and 2,4-D treatment in pea plants (Pazmiño 2009). Studies carried out *in vitro* and in animal cells have shown that actin is a major target of different post-translational modifications, such as oxidation and *S*-nitrosylation, and both processes triggered disturbances in actin polymerization giving rise to changes in cell morphology through the formation of multiple surface blebbs on the plasma membrane (Dalle-Donne *et al*., 2001). Similar changes in cell morphology have also been observed in pea leaves treated with 2,4-D (Pazmiño *et al*., 2011). Actin has several cysteines susceptible to redox modifications and also has several methionine susceptible to oxidation (Terman and Kashina, 2013). However, the role and hierarchical relationship between these post-translational modifications of actin under physiological and stress conditions have not being established so far (Terman and Kashina, 2013). The interplay between post-translational modifications of proteins has emerged as a very important regulatory mechanism (Sun *et al*., 2006; Lounifi *et al*., 2013). ROS and NO can compete for the same Cys residues to regulate proteins, and therefore can exert antagonistic roles. *S*-

nitrosylation has been suggested that can protect proteins to irreversibly carbonylation, and in its turn, irreversible oxidation of thiols can block the physiologic modification by *S*-nitrosylation (Sun *et al*., 2006; Lounifi *et al*., 2013). In addition to post-translational modification of actin in animal cells it has been reported that ROS can also disturb the actin cytoskeleton by activating mitogen-activated protein kinases, which lead to the phosphorylation of F-actin, affecting actin polymerization and cytoskeleton dynamics (Dalle-Donne *et al*., 2001; Foissner *et al*., 2002).

There is a cross-talk between auxins and actin, and a self-referring regulatory circuit between polar auxin transport and actin organization has been reported, although the mechanism is not well understood (Dhonukshe *et al*., 2008; Nick *et al*, 2009). Auxin transport inhibitors, such as 2,3,5-triiodobenzoic acid (TIBA) or sodium 4-phenylbutyrate (PBA), repress vesicle trafficking by influencing the actin cytoskeleton (Dhonukshe *et al*., 2008), and exogenous IAA regulates actin bundling, promoting the transformation of massive longitudinal bundles into finer strands (Nick *et al.*, 2009), although the mechanism involved in these changes of actin cytoskeleton have not been demonstrated. More recently, we have observed that brassinosteroids (BR) induced a wavy phenotype in Arabidopsis roots which was due to changes in the distribution of actin filaments and their dynamics (Lanza *et al*., 2012). NO can induce actin depolymerisation in sycamore tree cells treated with fusicoccin and this process has been associated also with the induction of programmed cell death (Malerba *et al*., 2008). ROS and NO also mediated the actin reorganization and the induction of programmed cell death in the pollen self-incompatibility response of *Papaver*, although the molecular mechanisms have not established so far (Wilkins *et al*., 2011). In this current work, we have demonstrated that 2,4-D does not induce degradation or down-regulation of actin and GFP-FABD2 but induces actin modifications by oxidation and *S*-nitrosylation, which affect the polymerization of F-actin prompting a strong reduction of actin organization. In animal cells, *S*-nitrosylation interferes with the normal state of F-actin, resulting in depolymerisation (Dalle-Donne *et al*., 2000). *S*-Nitrosylated G-actin polymerizes less efficiently than control actin and forms a lower amount of F-actin, compared to unmodified actin, which shortens the actin length distribution (Dalle-Donne *et al*., 2000). In maize roots, exogenous NO donors reportedly disturbed the actin

cytoskeleton and vesicle trafficking by reorganization of F-actin, and this effect was specific for cell type and developmental state (Kasprowicz *et al*., 2009).

The disturbances observed in the actin cytoskeleton could be responsible for the leaf epinasty induced by 2,4-D and, in fact, actin has been demonstrated to regulate the growth and the shape of leaf-epidermal pavement cells and trichomes (Smith & Oppenheimer, 2005), and has been found to be involved in growth alterations (Ketelaar *et al*., 2004). Baluska *et al*. (2001) have also observed that a reduction of the actin cytoskeleton induces cell radial growth resulting in them being shorter and wider which could explain the epinasty induced by 2,4-D observed in this work. In addition to this, the disturbances in the actin cytoskeleton promotes a reduction of the mobility and displacement of peroxisomes in response to 2,4-D. This effect was not specific for peroxisomes and the motility of mitochondria was also affected by 2,4-D. These disturbances could considerably affect the metabolism of these organelles because they share several metabolites with each other and with chloroplasts, and the disruption of their dynamics could compromise the metabolic pathways where they are involved. Thus, 2,4-D promotes reduction of carbon fixation, starch formation in plants (Grossmann, 2010) and affects mitochondrial respiration and fatty acid β-oxidation in yeast, animal and plant cells (Teixeira *et al*, 2007; Romero-Puertas *et al* 2004a; Grossmann, 2010). Peroxisomes contain a large battery of antioxidants and can participate in removing ROS from different parts of the cells and disturbances in their mobility could limit their role in antioxidative defence.

In conclusion, 2,4-D promotes oxidative stress, giving rise to post-translational changes of actin by oxidation and *S*-nitrosylation causing disturbances in the actin cytoskeleton, thereby affecting the dynamics and metabolism of peroxisomes and mitochondria. These structural changes in turn appear to be responsible for epinastic deformation of the leaf characteristic of this herbicide. Disturbances in the actin cytoskeleton could also affect vesicle trafficking and in general organelle movement giving rise to the metabolic disturbances and even further cell death after very long exposure to the herbicide (Fig. 6).

Supplementary Material

Figure S1: 2,4-D produces epinasty in Arabidopsis leaves and accumulation of H_2O_2 mainly in vascular tissue. Leaves were treated with 23 mM 2,4-D, and the effect were analysed after 72 h of treatment. A) 2,4-D induces leaf epinasty. B) Histochemical analysis of H_2O_2 production was carried out with DAB. Boxes show higher magnification of vascular tissue.

Figure S2: Imaging of $O_2^{\cdot-}$ production by CLSM using DHE (Ex/Em: 450-490/520 nm, green) and chlorophyll autofluorescence (red) showing magnifications of mesophyll cells from 2,4-D treated plants. A) $O_2^{\cdot-}$-dependent DHE fluorescence associated to secondary veins (SV), stomata (st) and epidermis (e). B) High magnification of a mesophyll cell showing DHE associated to small organelles (mitochondria and peroxisomes). C and D show the merge of $O_2^{\cdot-}$-dependent DHE fluorescence (green) and the chlorophyll autofluorescence (red, Ex/Em: 633/680 nm).

Figure S3: Histochemical staining with Trypan Blue from Arabiodospis leaves treated at different times with 2,4-D (23 mM). Leaves were stained with Trypan Blue as indicated in Materials and Methods. Bars= 200 μm.

Video S1A: Movies showing peroxisomal dynamics in epidermal cells from control *Arabidopsis* plants expressing the GFP-SKL.

Video S1B : Movies showing the effect of 23 mM 2,4-D on peroxisomal dynamics in epidermal cells from control *Arabidopsis* plants expressing the GFP-SKL.

Video S2A: Movies showing peroxisomal and mitochondrial dynamics in epidermal cells from control double markers *Arabidopsis* px-ck x mt-yk plants.

Video S2B: Movies showing the *effect* of 2,4-D on peroxisomal and mitochondrial dynamics in epidermal cells from double markers *Arabidopsis* px-ck x mt-yk plants.

Acknowledgements

D. Pazmiño and M. Rodríguez-Serrano acknowledge fellowships JAE-Pre and JAE-DOC, respectively from the CSIC and the European Social Fund (ESF). This work was supported by ERDF-cofinanced grants BIO2008-04067 and

BIO2012-36742 from MICINN and *Junta de Andalucía* (BIO-337), Spain. Authors acknowledge Dr D. McCurdy and Dr Sagi for providing the GFP-FABD2 and *xdh Arabidopsis* lines, respectively. We thank Dr T Ketelaar for critical reading. The confocal laser fluorescence microscopy analyses were carried out at the Technical Services of the University of Jaén and University of Granada.

Reference List

Astier J, Rasul S, Koen E, Manzoor H, Besson-Bard A, Lamotte O, Jendroz S, Durner J, Lindernayr C, Wendehenne D. 2011. S-nytrosylation: An emerging post-translational protein modification in plants. *Plant Science* **181:** 527-533

Baluska F, Jasik J, Edelmann HG, Salajová T, Volkmann D. 2001. Latrunculin B-induced plant dwarfism: Plant cell elongation is F-actin-dependent. *Developmental Biology* **231**:113-24.

Benjamins R, Scheres B. 2008. Auxin: The looping star in plant development. *Annual Review of Plant Biology* **59**: 443-465

Blume YB, Nyporko AY, Yemets AI, Baird WV. 2003. Structural modeling of the interaction of plant alpha-tubulin with dinitroaniline and phosphoroamidate herbicides. *Cell Biology International* **27:** 171-174

Collings DA, Lill AW, Himmelspach R, Wasteneys GO. 2006. Hypersensitivity to cytoskeletal antagonists demonstrates microtubule-microfilament cross-talk in the control of root elongation in *Arabidopsis thaliana*. *New Phytologist* **170**: 275-90.

Dalle-Donne I, Milzani A, Giustarini D, Di Simplicio P, Colombo R, Rossi R 2000. S-NO-actin: *S*-nitrosylation kinetics and the effect on isolated vascular smooth muscle. *Journal of Muscle Research and Cell Motility* **21**: 171-181

Dalle-Donne I, Rossi R, Milzani A, Di Simplicio P, Colombo R. 2001. The actin cytoskeleton response to oxidants: from small heat shock protein phosphorylation to changes in the redox state of actin itself. *Free Radical Biology & Medicine* **31:** 1624-1632

Delker C, Raschke A, Quint M 2008. Auxin dynamics: the dazzling complexity of a small molecule's message. *Planta* **227**: 929-941

Delledonne M 2005. NO news is good news for plants. *Current Opinion in Plant Biology* **8**: 390-396

Délye C, Menchari Y, Michel S, Darmency H. 2004. Molecular bases for sensitivity to Tubulin-Binding Herbicides in Green Foxtail. *Plant Physiology* **136:** 3920-3932

Dhonukshe P, Grigoriev I, Fischer R, Tominaga M, Robinson DG, Hasek J, Paciorek T, Petrasek J, Seifertova D, Tejos R, Meisel LA, Zazimalova E, Gadella TWJ, Jr., Stierhof Y-D, Ueda T, Oiwa K, Akhmanova A, Brock R,

Spang A, Friml J 2008. Auxin transport inhibitors impair vesicle motility and actin cytoskeleton dynamics in diverse eukaryotes. *Proceedings of the National Academy of Science* **105:** 4489-4494

del Río LA. 2011. Peroxisomes as a cellular source of reactive nitrogen species signal molecules. *Archives in Biochemistry and Biophysics* **506:** 1-11

Foissner I, Grolig F, Obermeyer G. 2002. Reversible protein phosphorylation regulates the dynamic organization of the pollen tube cytoskeleton: effects of calyculin A and okadaic acid. *Protoplasma* **220**: 1-5

Grossmann K. 2010. Auxin herbicides: current status of mechanism and mode of action. *Pest Managment Science* **66**: 113-120

Grossmann K, Kwiatkowski J, Tresch S.2001.Auxin herbicides induce H_2O_2 overproduction and tissue damage in cleavers (*Galiumaparine* L.). *Journal of Experimental Botany* **52:** 1811-1816

Halliwell B, Gutteridge JMC. 2000. Free radicals in biology and medicine, Oxford

Hussey PJ, Ketelaar T, Deeks MJ 2006. Control of the actin cytoskeleton in plant cell growth. *Annual Review of Plant Biology* **57**: 109 – 125

Jaffrey SR, Erdjument-Bromage H, Ferris CD, Tempst P, Snyder SH. 2001. Protein *S*-nitrosylation: a physiological signal for neuronal nitric oxide. *Nature Cell Biology* **3**: 193-197

Kasprowicz A, Szuba A, Volkmann D, Baluska F, Wojtaszek P 2009. Nitric oxide modulates dynamic actin cytoskeleton and vesicle trafficking in a cell type-specific manner in root apices. *Journal of Experimental Botany* **60**: 1605-1617

Ketelaar T, Allwood EG, Anthony RG, Voigt B, Menzel D, Hussey PJ. 2004. The actin-interacting protein AIP1 is essential for actin organization and plant development. *Current in Biol*ogy **14**: 57-62

Koch E, and Slusarenko A. 1990. Arabidopsis is susceptible to infection by a downy mildew fungus. *The Plant Cell* **2**: 437–445.

Lanza M, Garcia-Ponce B, Castrillo G, Catarecha P, Sauer M, Rodríguez-Serrano M, Páez-García, A, Sánchez-Bermejo E, Mohan TC, Leo del Puerto Y, Sandalio LM,Paz-Ares J, Leyva A. 2012. Role of actin cytoskeleton in brassinosteroid signaling and in its integration with the auxin response in plants. *Developmental Cell* **22:** 1275-1285

Liszkay A, van der Zalm E, Schopfer P. 2004. Production of reactive oxygen intermediates ($O2^{\cdot-}$, H_2O_2, and $^{\cdot}OH$) by maize roots and their role in wall loosening and elongation growth. *Plant Physiology* **136**: 3114-3123

Lounifi,I, Arc E, Molassiotis A, Job D, Rajjou,L, Tanou G 2013. Interplay between protein carbonylation and nitrosylation in plants. *Proteomics* **13**: 568–578

Malerba M, Contran N, Tonelli M, Crosti P, Cerana R. 2008. Role of nitric oxide in actin depolymerization and programmed cell death induced by fucicoccin in sycamore (*Acer pseudoplatanus*) culture cells. *Physiologia Plantarum* **133**: 449-467

Mano S, Nakamori C, Hayashi M, Kato A, Kondo M, Nishimura M. 2002. Distribution and characterization of peroxisomes in arabidopsis by visualization with GFP: dynamic morphology and actin- dependent movement. *Plant and Cell Physiology* **43**:331–341

Mittler R, Vanderauwera S, Suzuki N, Miller GAD, Tognetti VB, Vandepoele K, Gollery M, Shulaev V, Van Breusegem F. *2*011. ROS signaling: The new wave? *Trends in Plant Science***16**: 300-309

Moreau M, Lindermayr C, Durner J, Klessig DF. 2010. NO synthesis and signaling in plants- where do we stand? *Physiologia Plant*arum **138**: 372-383

Nakatsubo N, Kojima H, Kikuchi K, Nagoshi H, Hirata Y, Maeda D, Imai Y, Irimura T, Nagano T (1998) Direct evidence of nitric oxide production from bovine aortic endothelial cells using new fluorescence indicators: diaminofluoresceins. *FEBS Letters* **427:** 263-266

Neill S, Barros R, Bright J, Desikan R, Hancock J, Harrison J, Morris P, Ribeiro D, Wilson I. 2008. Nitric oxide, stomatal closure, and abiotic stress. *Journal of Experimental Botany* **59**: 165-176

Nelson BK, Cai X, Nebenführ A . 2007. A multicolored set of in vivo organelle markers for co-localization studies in Arabidopsis and other plants. *Plant Journal* **51:** 1126-1136.

Nick P, Han MJ, An G. 2009. Auxin stimulates its own transport by shaping actin filaments. *Plant Physiol*ogy **151**: 155-167

Ortega-Galisteo A, Rodríguez-Serrano M, Pazmino DM, Gupta D, Sandalio LM, Romero-Puertas MC. 2012. S-nitrosylated proteins in pea (*Pisum sativum*

L.) leaf peroxisomes: changes under abiotic stress. *Journal of Experimental Botany* **63**: 2089-2103.

Ovidi E, Gambellini G, Taddei AR, Cai G, Del Casino C, Ceci M, Rondini S, Tiezzi A 2001. Herbicides and the microtubular apparatus of *Nicotiana tabacum* pollen tube: Immunofluorescence and immunogold labelling studies. *Toxicology in Vitro* **15**: 143-151

Pazmiño DM 2009. Contribución de las especies de oxígeno y nitrógeno reactivo, y de los peroxisomas a la toxicidad del 2,4-D en plantas. PhD Thesis. University of Granada, Spain

Pazmiño DM, Rodríguez-Serrano M, Romero-Puertas MC, Archilla-Ruiz A, Del Río LA, Sandalio LM. 2011. Differential response of young and adult leaves to herbicide 2,4-dichlorophenoxyacetic acid in pea plants: role of reactive oxygen species. *Plant &Cell Environment* **34**: 1874-1889

Pazmiño DM, Romero-Puertas MC, Sandalio LM. 2012. Insights into the toxicity mechanism of and cell response to the herbicide 2,4-D in plants. *Plant Signaling and Behaviour* **7**: 1-3

Pazmiño DM, Rodríguez-Serrano M, Sanz M, Romero-Puertas MC & Sandalio LM 2014 Regulation of epinasty induced by 2,4-dichlorophenoxyaceticacid in pea and *Arabidopsis* plants. *Plant Biology*, doi: 10.1111/plb.12128.

Rahman A, Bannigan A, Sulaman W, Pechter P, Blancaflor EB, Baskin TI. 2007. Auxin, actin and growth of the *Arabidopsis thaliana* primary root. *Plant Journal* **50:** 514-528

Rasmussen I, Pedersen LH, Byg L, Suzuki K, Sumimoto H, Vilhardt F. 2010. Effects of F/G-actin ratio and actin turn-over rate on NADPH oxidase activity in microglia. *BMC Immunology* **11**:44 doi:10.1186/1471-2172-11-44

Rodríguez-Serrano M, Romero-Puertas MC, Sparkes I, Hawes C, del Río LA, Sandalio LM. 2009. Peroxisome dynamics in Arabidopsis plants under oxidative stress induced by cadmium. *Free Radical in Biology & Medicine* **47**: 1632-1639

Romero-Puertas MC, Palma JM, Gómez M, del Río LA, Sandalio LM. 2002. Cadmium causes the oxidative modification of proteins in pea plants. *Plant, Cell & Environment* **25**: 677-686

Romero-Puertas MC, McCarthy I, Gómez M, Sandalio LM, Corpas FJ, del Río LA, Palma JM. 2004a. Reactive oxygen species-mediated enzymatic systems involved in the oxidative action of 2,4-dichlorophenoxyacetic acid. *Plant, Cell & Environment* **27**: 1135-1148

Romero-Puertas MC, Rodríguez-Serrano M, Corpas FJ, Gómez M, del Río LA, Sandalio LM. 2004b. Cadmium-induced subcellular accumulation of $O_2^{\cdot-}$ and H_2O_2 in pea leaves. *Plant Cell &Environment* **27**: 1122-1134

Romero-Puertas MC, Rodríguez-Serrano M, Sandalio LM. 2013. Protein S-nitrosylation in plants under abiotic stress: an overview. *Frontiers in Plant Science*. **4**: 373.

Sandalio LM, Rodríguez-Serrano M, Romero-Puertas MC, del Río LA. 2008. Imaging of reactive oxygen species and nitric oxide in vivo in plant tissues. *Methods in Enzymo*logy **440**: 397-409

Sandalio LM, Rodríguez-Serrano M, Gupta DK, Archilla A, Romero-Puertas MC, del Río LA. 2012. Reactive Oxygen Species and Nitric Oxide in Plants Under Cadmium Stress. In: *Toxicity to Signaling*. Environmental Adaptations and Stress Tolerance of Plants in the Era of Climate Change (Amad P, Prassad MNV, Eds,) 199-215

Sandalio L.M., Rodríguez-Serrano M., Romero-Puertas M.C., del Río L.A. (2013) Role of peroxisomes as a source of reactive oxygen species (ROS) signaling molecules. In: del Río LA, ed. *Peroxisomes and their Key Role in Cellular Signaling and Metabolism*. Springer Science+Busines, Dordrecht, pp 231-249.

Schopfer P, Liszkay A, Bechtold M, Frahry G, Wagner A 2002. Evidence that hydroxyl radicals mediate auxin-induced extension growth. *Planta* **214**: 821-828

Sheahan MB, Staiger JC, RoseRJ, McCurdy DW. 2004. A green fluorescent protein fusion to actin-binding domain 2 of Arabidopsis fimbrin highlights new features of a dynamic actin cytoskeleton in live plant cells. *Plant Physio*logy **136**: 3968-3978

Sheremet YA, Yemets AI, Blume YB. 2012. Inhibitors of tyrosine kinases and phosphatases as a tool for the investigation of microtubule role in plant cold response. *Cytology and Genetic* **46**: 1-8

Smith LG, Oppenheimer DG. 2005. Spatial control of cell expansion by the plant cytoskeleton. *Annual Review of Cell and Developmental Biology* **21**: 271-294

Song X, Ma Q, Hao X, Li H. 2012. Roles of the actin cytoskeleton and an actin-binding protein in wheat resistance against *Puccinic striiformis* f. sp. *tritici*. *Protoplasma* **249**: 99-106

Staiger CJ, Blanchoin L. 2006. Actin dynamics: old friends with new stories. *Current Opinion in Plant Bi*ology **l9**: 554-562

Staiger CJ, Sheahan MB, Khurana P, Wang X, McCurdy DW, Blanchoin L. 2009. Actin filament dynamics are dominated by rapid growth and severing activity in the Arabidopsis cortical array S. *Journal of Cell Biology* **184**: 269-280

Stamler JS, Lamas S, Fang FC 2001.Nitrosylation, the prototypic redox-based signaling mechanism. *Cell* **106:** 675-683

Sun J, Steenbergen C, Murphy E 2006 S-nitrosylation: NO-related redox signaling to protect against oxidative stress. *Antioxidants & Redox Signaling* **8:** 1693-1705

Suzuki N, Koussevitzky S, Mittler R, Miller G 2011. ROS and redox signalling in the response of plants to abiotic stress. *Plant, Cell & Environment* **35**: 259-270

Teixeira MC, Duque P, Sá-Correia 2007. Environmental genomics: mechanistic insights into toxicity of and resistance to the herbicide 2,4-D. *Trends in Biotechnology*, **25**: 363-370

Terman JR, Kashina A 2013 Post-translational modification and regulation of actin. *Current Opinion in Cell Biology* **25**:30–38

Vandenabeele S, Vanderauwera S, Vuylsteke M, Rombauts S, Langebartels C., Seidlitz HK, Zabeau M, Van Montagu M, Inzé D & Van Breusegem F (2004) Catalase deficiency drastically affects gene expression induced by high light in Arabidopsis thaliana. *The Plant Journa*l **39**,:45–58

Vandelle E, Delledonne M. 2011. Peroxinitrite formation and function in plants. *Plant Science* **181**: 534-539

Van Gestel K, Kohler RH, Verbelen JP. 2002. Plant mitochondria move on F-actin, but their positioning in the cortical cytoplasm depends on both F-actin and microtubules. *Journal of Experimental Botany* **53:**659–667.

Wasteneys GO, Yang Z. 2004. New views on the plant cytoskeleton. *Plant Physiology* **136**: 3884-3891

Wilkins KA, Bancroft J, Bosch M, Ings J, Smirnoff N, Franklin-Tong VE. 2011. Reactive oxygen species and nitric oxide mediate actin reorganization and programmed cell death in the self-incompatibility response of *Papaver*. *Plant Physiology* **156**: 404–416.

Yemets AI, Kraslylenko YA, Lytryn DI, Sheremet YA, Blume YB. 2011. Nitric oxide signalling via cytoskeleton in plants. *Plant Science* **181**: 545-554.

Zaninotto F, Camera SL, Polverari A, Delledonne M. 2006. Cross talk between reactive nitrogen and oxygen species during the hypersensitive disease resistance response. *Plant Physiol*ogy **141**: 379-383.

Figure legends

Figure 1. Effect of 2,4-D and EDTA on Arabidopsis phenotype. A) Plants were treated once by foliar application of 23 mM 2,4-D and the effect on phenotype was followed at different period of treatment (1 h-72 h). Pictures correspond to the same plant at different time of treatment. B) Effect of EDTA (10 mM) on 2,4-D-induced phenotype. Plants were sprayed with EDTA before treatment with 2,4-D and the effect was analysed after 72h of treatment.

Figure 2. Imaging and quantification of H_2O_2, $O_2^{\cdot -}$ and NO production induced by the treatment with 2,4-D in *Arabidopsis thaliana* leaves. A) H_2O_2 content was analysed in acid extracts from Arabidopsis leaves by fluorimetry. Values are means±SE of four different experiments with three independent extracts each. B) Imaging of H_2O_2 accumulation in cross-sections of Arabidopsis leaves by CLSM using DCF-DA (Ex/Em: 485/530 nm). DCF-DA fluorescence was quantified in arbitrary units (C). D, E) Imaging and quantification of $O_2^{\cdot -}$ production using DHE (Ex/Em: 450-490/520 nm. F, G) Imaging and quantification of NO production using DAF-2DA (Ex/Em: 495/515nm). cPTIO was used as a NO scavenger. H) NO content was quantified in arbitrary units (a.u.) in leaf extracts from Arabidopsis leaves by fluorimetry. Images are maximal projections from several optical sections and are representative of at least 15 leaf sections from four different experiments. Different letters indicate significant difference at $P< 0.05$ as determined by Duncan´s multiple-range test. e, epidermis; mc, mesophyll cells; st, stomata; x, xylem.

Figure 3. Effect of 2,4-D on actin cytoskeleton in epidermal cells of Arabidopsis leaves. A) Arabidopsis plants expressing the fusion protein GFP-FABD2 were used to visualize the effect of 2,4-D (23 mM) on actin cytoskeleton at different time of treatment. B) Effect of EDTA (10 mM) and 2,4-D on actin cytoskeleton after 72 h of treatment. C) Effect of Latrunculin B (Lat B; 25 μM) on actin cytoskeleton. Fluorescence for each treatment was quantified as mentioned in Materials and Methods and expressed in arbitrary units. The mean±SE of at least 10 leaf sections from three different experiments is shown inside the panels. Data followed by the same latter are not statistically different according to Duncan's multiple-range test. Bars represent 25 μm in A and B, and 5 μm in C. D) Effect of 2,4-D on the rate F-ACT/G-ACT over the treatment analysed by Western blot

of proteins using anti-actin antibodies. Equal volume of proteins was used for each fraction. E) GFP-FABD2 expression in leaves after 72 h of treatment analysed by Western blot of proteins using a specific anti-GFP antibody. Equal amount of protein was loaded per well. F) Variation in total ACT protein accumulation in WT plants after 72 h of treatment with 2,4-D and EDTA and in *Atxdh* plants monitored by Western blot analysis using a specific anti-actin antibody. Equal amount of protein was loaded per well.

Figure 4. Analysis of post-translational modifications of actin by carbonylation and *S*-nitrosylation. A) Detection of carbonylated actin. Proteins from leaf extracts (500 μg) were derivatized with DNPH and immunoprecipitated with anti-DNP-IPA as indicated in Materials and Methods. Oxidized-purified proteins (10 μl) were subjected to SDS-PAGE, transferred onto PVDF membranes and analysed with an anti-actin antibody. The Figure is representative of four independent experiments. B) Detection of *S*-nitrosylated actin. *S*-nitrosylated proteins were labeled with biotin and Immunopurified with anti-biotin-IPA, individualized by SDS-PAGE and the actin was identify by Western blot analysis using an anti-actin antibody. The Figure is representative of three independent experiments.

Figure 5. Effect of 2,4-D on peroxisome dynamics in epidermal cells. Seedlings expressing GFP-SKL were treated with 23 mM 2,4-D with or without 10 mM EDTA for 72 h. The speed (A) and displacements (B) were studied by time-lapse analysis using a confocal laser microscope and the images obtained were processed using Volocity3 software. Results are means±SE of three different parts of the leaf, and at least ten different plants from three different experiments were used. Values with different letters are significant different ($P<0.05$) as determined by Duncan´s multiple-range test.

Figure 6. Schematic showing the possible mechanistic toxicity of 2,4-D in Arabidopsis plants. 2,4-D promotes oxidative stress, where peroxisomes and mitochondria represent the main sources of ROS, giving rise to post-translational changes of actin by oxidation and *S*-nitrosylation causing disturbances in the actin cytoskeleton, thereby affecting trafficking of organelles. These structural changes in turn appear to be responsible for leaf epinasty, although processes involved in developing epinasty also can contribute to actin cytoskeleton disturbances. Alteration of cytoskeleton could also be responsible for metabolic

disturbances, signalling disruption and further senescence. XDH, xanthine dehydrogenase; ACX, acyl CoA oxidase.

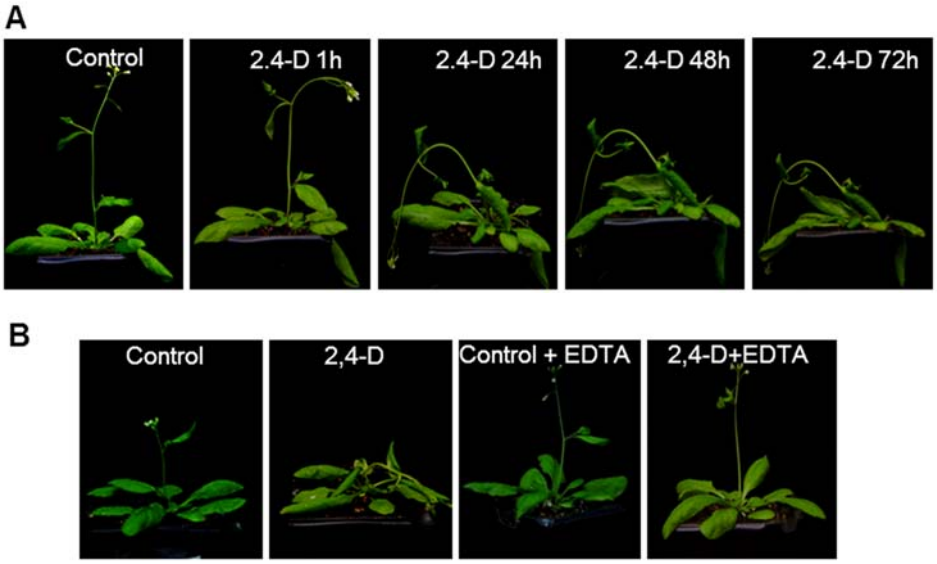
A
Control
2.4-D 1h
2.4-D 24h
2.4-D 48h
2.4-D 72h
B
Control
2,4-D
Control + EDTA
2,4-D+EDTA

Figure 1

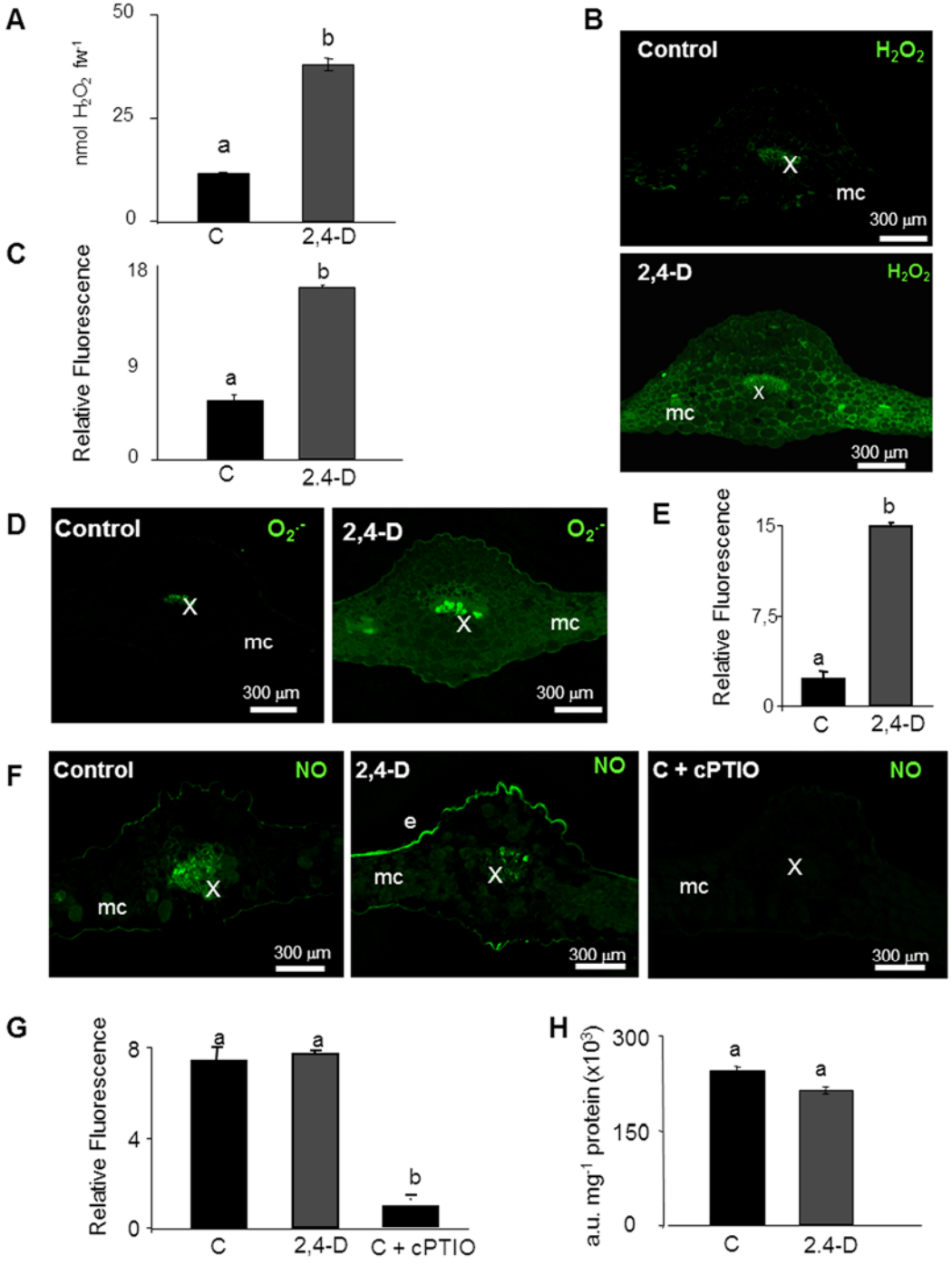
A
nmol H_2O_2 fw^{-1}
50
25
0
a
b
C
2,4-D
B
Control
H_2O_2
X
mc
300 µm
2,4-D
H_2O_2
X
mc
300 µm
C
Relative Fluorescence
18
9
0
a
b
C
2,4-D
D
Control
$O_2^{\cdot-}$
X
mc
300 µm
2,4-D
$O_2^{\cdot-}$
X
mc
300 µm
E
Relative Fluorescence
15
7,5
0
a
b
C
2,4-D
F
Control
NO
X
mc
300 µm
2,4-D
NO
e
mc
X
300 µm
C + cPTIO
NO
X
mc
300 µm
G
Relative Fluorescence
8
4
0
a
a
b
C
2,4-D
C + cPTIO
H
a.u. mg^{-1} protein (x10^3)
300
150
0
a
a
C
2.4-D

Figure 2

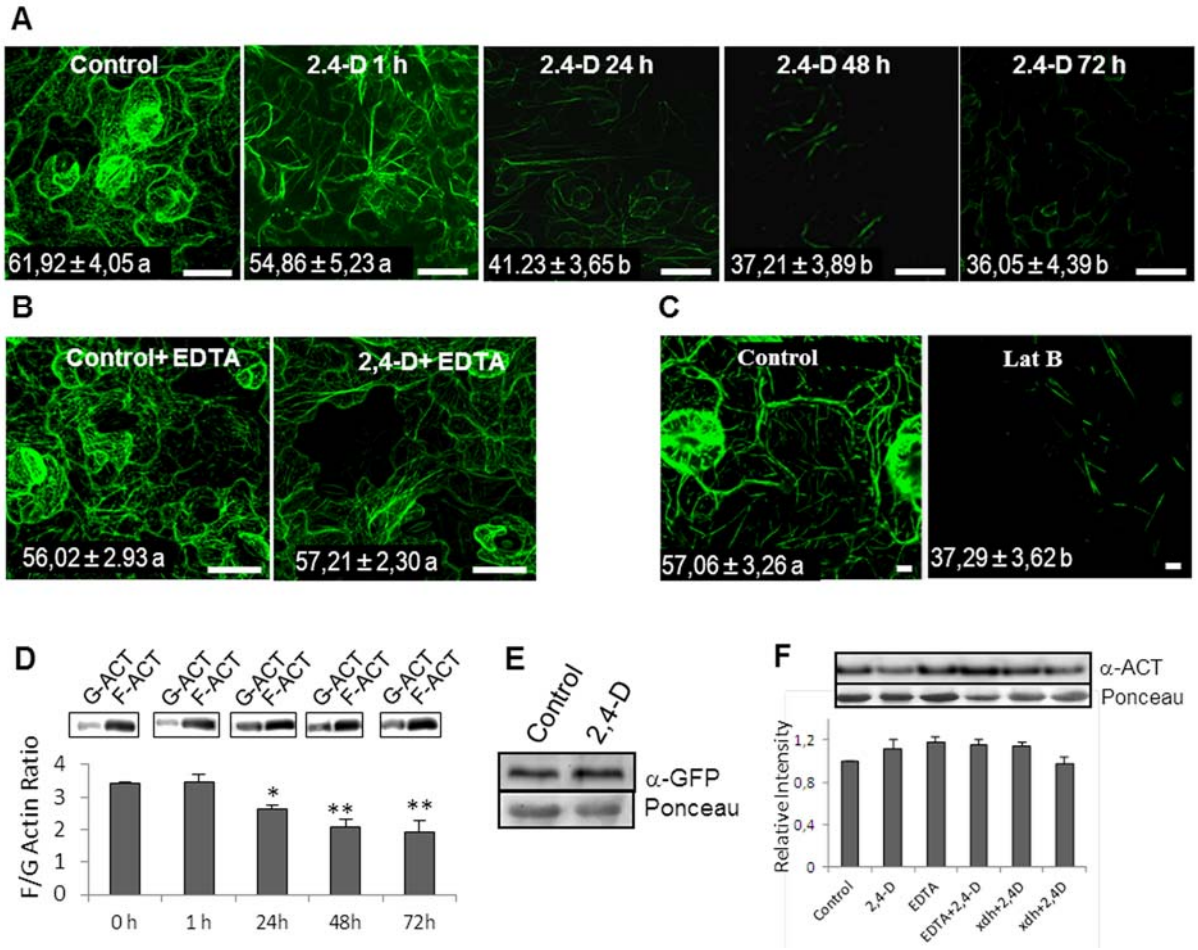
A
Control
2.4-D 1 h
2.4-D 24 h
2.4-D 48 h
2.4-D 72 h
61,92 ± 4,05 a
54,86 ± 5,23 a
41.23 ± 3,65 b
37,21 ± 3,89 b
36,05 ± 4,39 b
B
Control+ EDTA
2,4-D+ EDTA
56,02 ± 2.93 a
57,21 ± 2,30 a
C
Control
Lat B
57,06 ± 3,26 a
37,29 ± 3,62 b
D
G-ACT
F-ACT
F/G Actin Ratio
0 h
1 h
24h
48h
72h
E
Control
2,4-D
α-GFP
Ponceau
F
α-ACT
Ponceau
Relative Intensity
Control
2,4-D
EDTA
EDTA+2,4-D
xdh+2,4D
xdh+2,4D

Figure 3

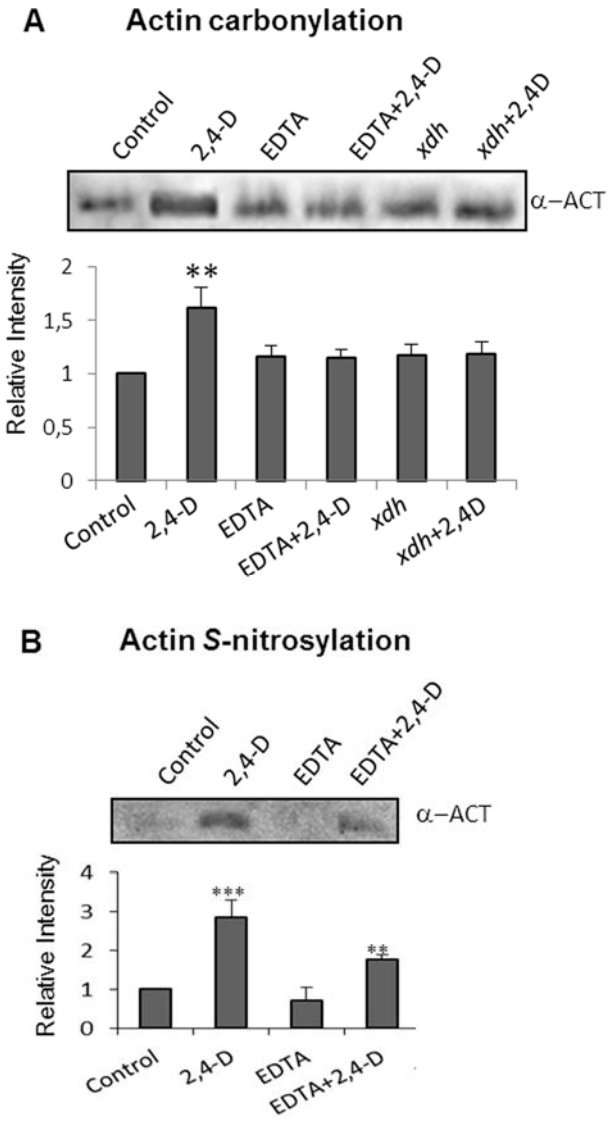
A
Actin carbonylation
Control
2,4-D
EDTA
EDTA+2,4-D
xdh
xdh+2,4D
α–ACT
Relative Intensity
2
1,5
1
0,5
0
**
Control
2,4-D
EDTA
EDTA+2,4-D
xdh
xdh+2,4D
B
Actin S-nitrosylation
Control
2,4-D
EDTA
EDTA+2,4-D
α–ACT
Relative Intensity
4
3
2
1
0
***
**
Control
2,4-D
EDTA
EDTA+2,4-D

Figure 4

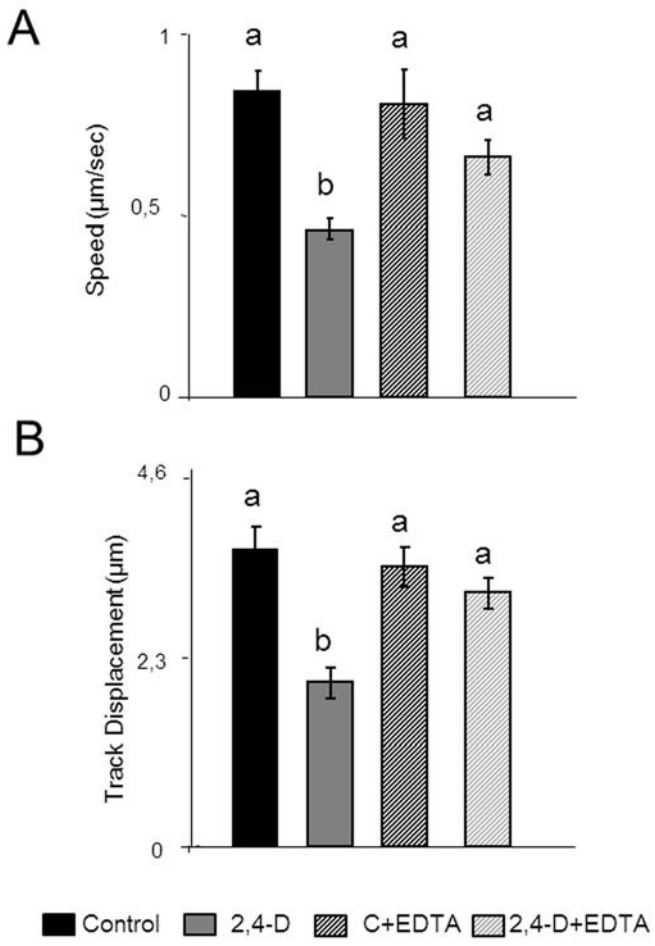
A
1
0,5
0
Speed (µm/sec)
a
b
a
a
B
4,6
2,3
0
Track Displacement (µm)
a
b
a
a
Control
2,4-D
C+EDTA
2,4-D+EDTA

Figure 5

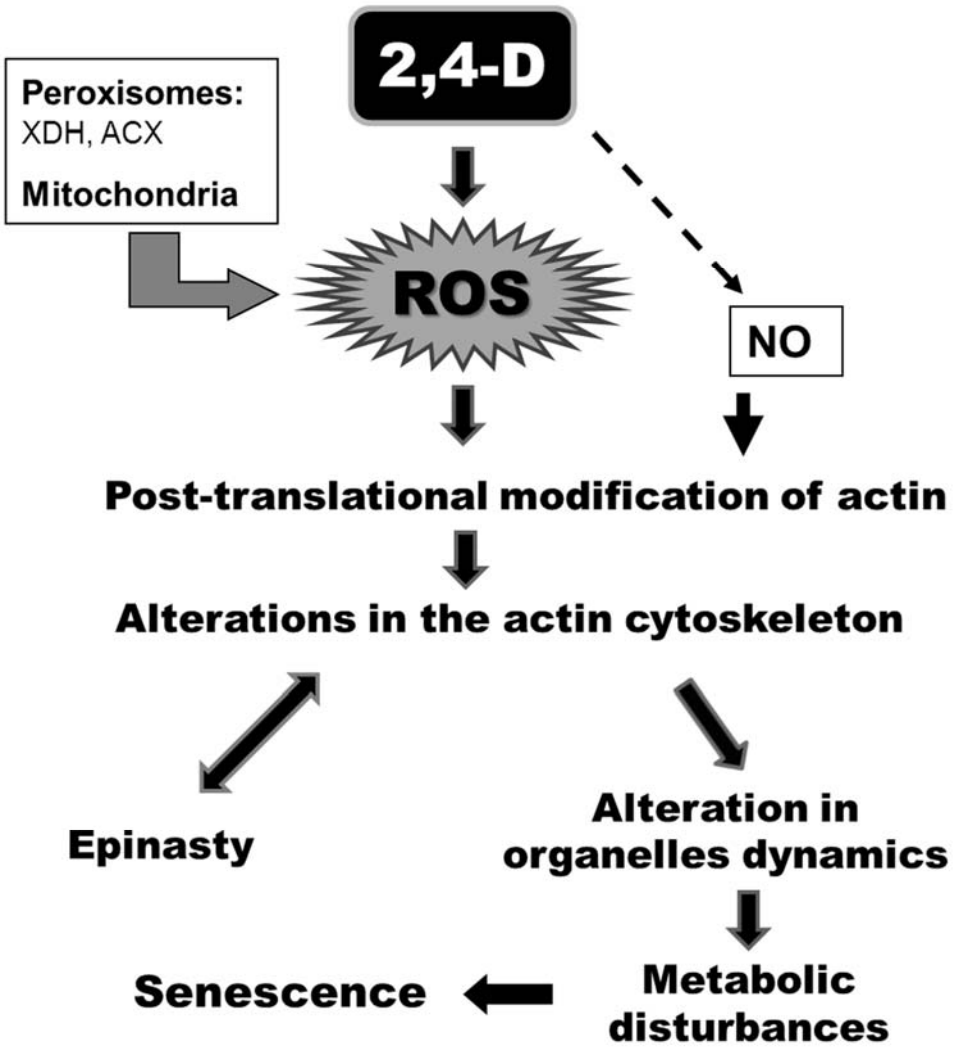
2,4-D
Peroxisomes:
XDH, ACX
Mitochondria
ROS
NO
Post-translational modification of actin
Alterations in the actin cytoskeleton
Epinasty
Alteration in
organelles dynamics
Senescence
Metabolic
disturbances

Figure 6